Virology 450-451 (2014) 182–195

Contents lists available at ScienceDirect

Virology

journal homepage: www.elsevier.com/locate/yviro

MicroRNA-23 inhibits PRRSV replication by directly targeting PRRSV RNA and possibly by upregulating type I interferons

Qiong Zhang [a,b,c], Xue-kun Guo [a,b,c], Li Gao [a,b,c], Chen Huang [a,b,c], Ning Li [a,d], Xiaojuan Jia [e], Wenjun Liu [e], Wen-hai Feng [a,b,c,*]

[a] State Key Laboratory of Agrobiotechnology, College of Biological Sciences, China Agricultural University, Beijing 100193, China
[b] Ministry of Agriculture Key Laboratory of Soil Microbiology, College of Biological Sciences, China Agricultural University, Beijing 100193, China
[c] Department of Microbiology and Immunology, College of Biological Sciences, China Agricultural University, Beijing 100193, China
[d] Department of Molecular Biology, College of Biological Sciences, China Agricultural University, Beijing 100193, China
[e] Institute of Microbiology, Chinese Academy of Sciences, Beijing 100101, China

ARTICLE INFO

Article history:
Received 18 September 2013
Returned to author for revisions
19 October 2013
Accepted 17 December 2013
Available online 4 January 2014

Keywords:
PRRSV
microRNAs
miR-23
miR-378
miR-505
IFNs
IRF

ABSTRACT

MicroRNAs (miRNAs) are small non-coding RNAs that regulate gene expression post-transcriptionally and play critical roles in intricate networks of host–pathogen interactions and innate immunity. Porcine reproductive and respiratory syndrome (PRRS) is one of the most important diseases affecting swine industry worldwide. Here, we demonstrated that miR-23, miR-378, and miR-505 were antiviral host factors against PRRS virus (PRRSV). Over-expression of the three miRNAs inhibited PRRSV infection in a dose-dependent manner, respectively. Blockage of the three endogenously expressed miRNAs significantly enhanced PRRSV replication. Different type 2 PRRSV strains harbored conserved miR-23, miR-378, and miR-505 target sites (TSs) that were sufficient to confer miRNA-mediated repression of PRRSV replication. Interestingly, miR-23 was capable of inducing type I interferon expression during PRRSV infection through IRF3/IRF7 activation, which might further lead to the inhibition of virus infection. These results suggest that miR-23, miR-378, and miR-505, especially miR-23, may have the potential to be used as antiviral therapy against PRRSV infection.

Introduction

Porcine reproductive and respiratory syndrome (PRRS) is one of the most important diseases in swine industry worldwide, and has been causing significant economic losses since it was first reported in the United States and Canada in 1987 (Wensvoort et al., 1992). Porcine reproductive and respiratory syndrome virus (PRRSV), the etiological agent of the disease, is an enveloped, positive-sense, and single-stranded RNA virus belonging to the *Arteriviridae* family within the order *Nidovirales* (Cavanagh, 1997). PRRSV includes two major genotypes, the European type (type 1) and the North American type (type 2) (Allende et al., 1999). The PRRSV genome is about 15.4 kb in length, containing at least two large replication-related genes (ORF1a and ORF1b), and eight structural protein genes (GP2a, GP2b, GP3, GP4, GP5a, GP5b, the matrix protein M, and the nucleocapsid N protein) (Firth et al., 2011; Johnson et al., 2011).

MicroRNAs (miRNAs) are small (~23 nt) non-coding RNAs that regulate gene expression post-transcriptionally through degradation of mRNAs or inhibition of translation (Bartel, 2009). The RNA-induced silencing complex (Rani et al., 2011) is the core miRNA-mediated silencing machinery, where miRNA serves as a guide RNA to target mRNAs bearing the complementary sequence. The complementarity between the miRNA 'seed region' (positions 2–8 from the 5′ end) and the sequence of the mRNA target is considered to be critical for the specificity of miRNA-target mRNA interaction (Carthew and Sontheimer, 2009). Yet specificity of the miRNA is also influenced by other factors such as the presence and cooperation between multiple target sites (TSs), the spacing between TSs, proximity to the stop codon, position within the mRNA, AU composition, and the target mRNA secondary structure (Bartel, 2009; Shukla et al., 2011).

Mounting evidence suggests a complicated interplay between viruses and miRNAs. On the one hand, a virus can exploit the miRNA system to facilitate its replication (Gottwein et al., 2007). On the other hand, multiple miRNAs in hosts have been identified as inhibitors of viral replications by directly targeting viral genomes (Huang et al., 2007; Otsuka et al., 2007; Song et al., 2010; Zheng et al., 2013) or inhibiting factors necessary for viral life cycles (Ouda et al., 2011; Triboulet et al., 2007). Additionally, host

* Corresponding author at: State Key Laboratory of Agrobiotechnology, Department of Microbiology and Immunology, College of Biological Sciences, China Agricultural University, Beijing 100193, China.
Tel: +86 10 62733335, fax: +86 10 62732012.
E-mail address: whfeng@cau.edu.cn (W.-h. Feng).

0042-6822/$ - see front matter © 2013 Elsevier Inc. All rights reserved.
http://dx.doi.org/10.1016/j.virol.2013.12.020

Table 1
Target sites prediction of 12 candidate miRNAs and conservation analysis on 168 PRRSV strains of target sites.

Candidate miRNAs					
	Predicted seed-matched target sites in the viral RNA (miRNA seed sequences and the corresponding target sites are underlined and bolded)	Predicted seed-matched target sites in the viral RNA	Seed match	Conservation **(identity)** in type 2	Conservation **(identity)** in type 1
miR-23	ORF 3: 5'-TATTTGGGATAGGG**AATGTGA**G-3' miR-23: 3'-CCUUUAGGGACCG**UUACACU**A-5'	ORF3	7mer-m8	98.13%	86.62%
miR-505	ORF 3: 5'-ATGTGAGTCAAGTTTA**TGTTGACA**-3' miR-505: 3' -UCCUUUGGUCGUUC**ACAACUG**C -5' ORF 5: 5'- TGTCATCTTCCCCG**TGTTGAC**T -3' miR-505: 3' -UCCUUUGGUCGUUC**ACAACUG**C -5'	ORF3; ORF5	8mer; 7mer-m8	95.00%; 81.25%	0.00%
miR-378	ORF 7: 5'-GCCCAACAAAACC**AGTCCAGA** -3' miR-378: 3' -GGAAGACUGAGGU**UCAGGUC**A- 5'	ORF7	8mer	96.84%	0.00%

miR-106/93	ORF 6: 5'-ACATGACATTCGT**GCACTTT**C -3' miR-106: 3' -GAUGGACGUGACAUU**CGUGAAA**A5'	ORF6	7mer-m8	93.67%	7.69%
miR-128	ORF 7 : 5' - AGGGAGGATAAGTTA**CACTGTG**G -3' miR-128 : 3'-UUUCUCUGGCCAA**GUGACAC**U -5' 3'UTR 5' - AATGGCACTGATTGA**CACTGTG**C-3' miR-128 : 3'-UUUCUCUGGCCAA**GUGACAC**U -5'	ORF7; 3'UTR	7mer-m8	91.875%; 93.125%	46.15%
miR-107	ORF 2: 5'- TGGCTTCCCGGCTACCC**ATGCTGCA**-3' miR-107 : 3'-ACUAUCGGGACAUGU**UACGACG**A -5'	ORF2	8mer/7mer-m8	65.19%	0.00%
miR-34	ORF 4: 5'-TACATCACCAT**CACTGCC**A -3' miR-34 : 3'-UGUUGGUCGAUUCU**GUGACGG**U -5' ORF 1: 5'-GTGGTGAGCGAGGCCA**CACTGTC**T -3' miR-34 : 3'-UGUUGGUCGAUUCU**GUGACGG**U -5'	ORF4; ORF1	8mer; 7mer-m8	62.66%; 76.25%	0.00%

miR-146	ORF 4:5'-CTCTCCGGCGATTCGCAAA**AGTTCTC**A -3' miR-146 : 3'-UCGGAUACCUUAAG**UCAAGAG**U -5' ORF 1: 5'-CTGGCGTGCGCGG**AGTTCTC**G -3' miR-146 : 3'-UCGGAUACCUUAAG**UCAAGAG**U -5'	ORF4; ORF1	7mer-m8; 7mer-m8	51.90%; 95.00%	0.00%
miR-223	ORF 1: 5'-AACGTCGACGGCG**AACTGAC**T -3' miR-223 : 3'-ACCCCAUAAACUGU**UUGACUG**U -5'	ORF1	7mer-m8	88.00%	0.00%
miR-15	ORF 1: 5'-GTCAAGTTATTGAGGAT**TGCTGCT**G -3' miR-15 : 3'-GUGUUUGGUAAUAC**ACGACGA**U-5'	ORF1	7mer-m8	90.00%	46.15%
miR-16	ORF 1: 5'-GTCAAGTTATTGAGGAT**TGCTGCT**G -3' miR-16 : 3'-GCGGUUAUAAAUGC**ACGACGA**U-5'	ORF1	7mer-m8	90.00%	46.15%
miR-101	ORF 1: 5'-CTTAAGAAACA**GTACTGT**G -3' miR-16 : 3'-AAGUCAAUAGUGU**CAUGACA**U-5'	ORF1	7mer-m8	94.375%	0.00%

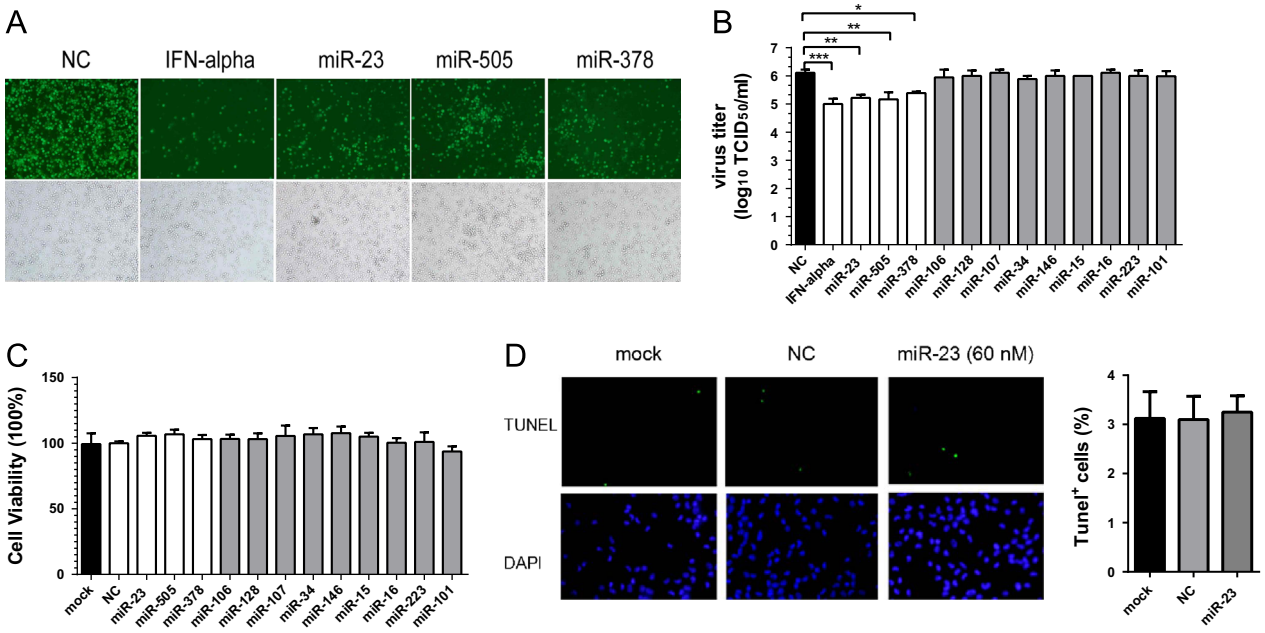

Fig. 1. miR-23, miR-505, and miR-378 inhibit PRRSV replication. PAMs were transfected with mimics of the indicated miRNAs or negative control miRNA mimics (NC) for 24 h at the concentration of 60 nM, and then infected with JXwn06 strain for 48 h at a multiplicity of infection (MOI) of 0.01. (A) Cells were fixed for immunofluorescent analysis of PRRSV N protein. Three miRNAs (miR-23, miR-505, and miR-378) showing efficient inhibitory abilities were presented. (B) Culture supernatants were simultaneously collected for virus titer analysis on PAMs. IFN-α was incubated 24 h at 100 U/ml before PRRSV infection, which served as positive control. (C) Transfection of miRNAs has no effect on cell viability. MTT assay was performed on PAMs transfected with mimics of the indicated miRNAs or NC for 72 h at the concentration of 60 nM. Data were representative of three independent experiments (mean ± SD). (D) Apoptosis could not be induced by transfection of miR-23 mimics into PAMs. TUNEL analysis of apoptosis was performed in PAMs either left untreated or transfected with 60 nM miR-23 or NC mimics for 72 h. Then, apoptosis (green, TUNEL positive) was detected. Statistical significance in B and C was analyzed by one-way ANOVA followed by post hoc Dunnett's multiple comparison. Significance compared to NC and mock-baseline, respectively: $^{*}P<0.05$; $^{**}P<0.01$; $^{***}P<0.001$. Statistical significance in D was analyzed by *t*-test.

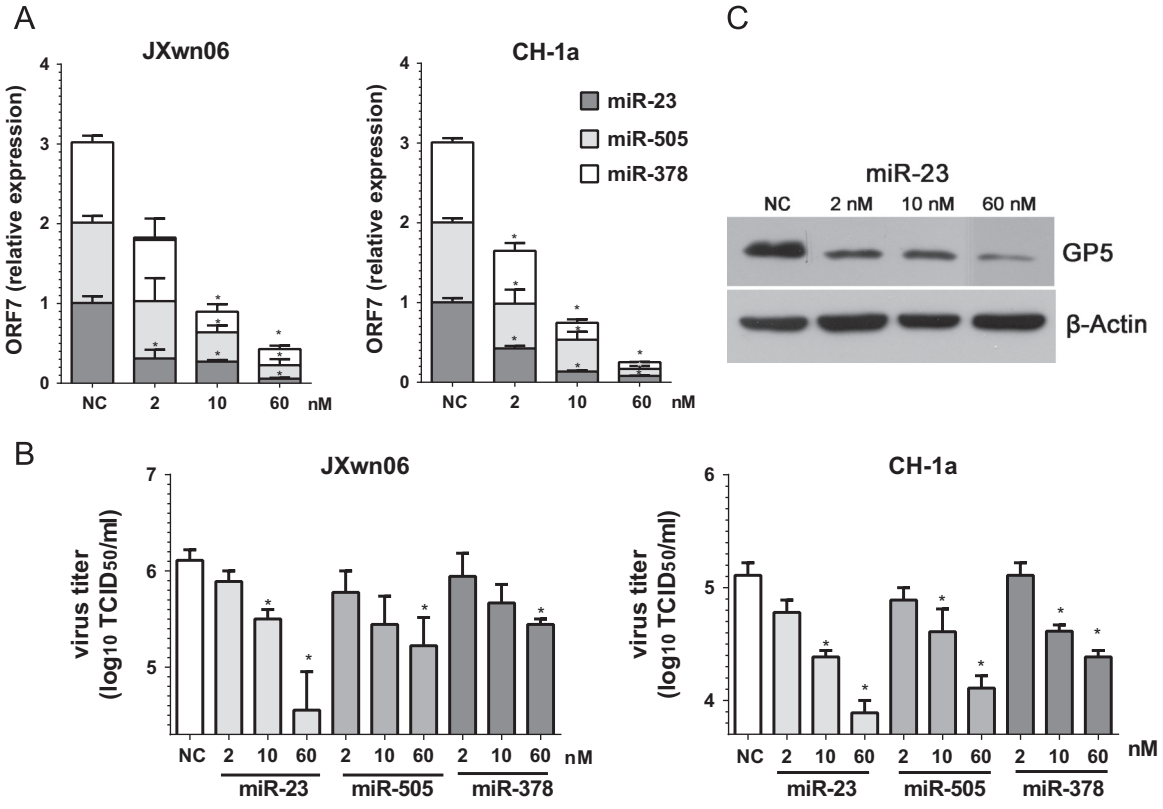

Fig. 2. miR-23, miR-505, and miR-378 suppress both JXwn06 and CH-1a replication dose-dependently. PAMs and Marc-145 cells were transfected with miR-23, miR-505, or miR-378 mimics at the indicated doses (2 nM, 10 nM, and 60 nM), and cells were then infected with JXwn06 or CH-1a PRRSV strains (MOI = 0.01) 24 h after transfection. Cells were collected 48 h (JXwn06) or 36 h (CH-1a) later for qRT-PCR analysis of ORF7 expression (normalized to GAPDH) (A), and viral yields in the supernatants were also quantified (B). (C) The levels of PRRSV protein GP5 were analyzed by Western blot. Expression of β-actin was shown as a loading control. Data were representative of three independent experiments (mean ± SD). Statistical significance was analyzed by *t*-test; $^{*}P<0.05$.

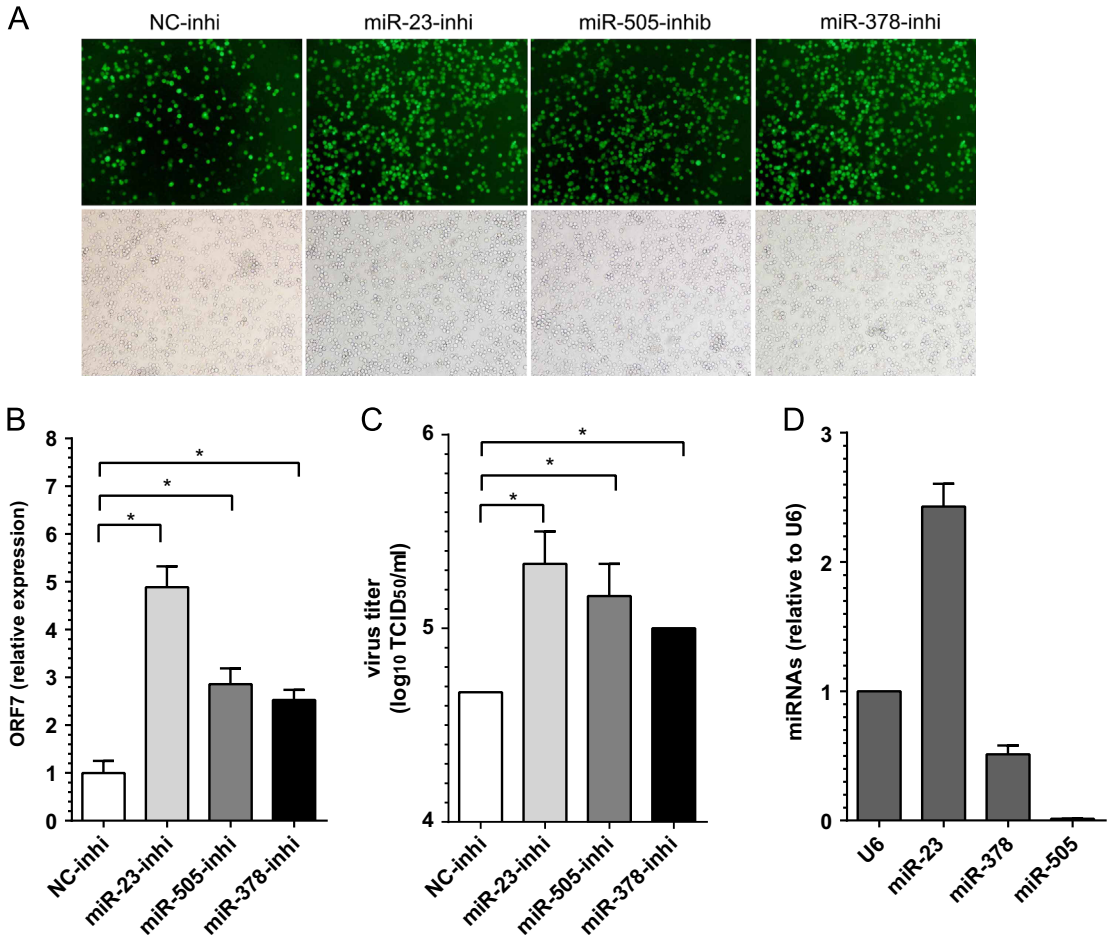

Fig. 3. Inhibition of endogenous miR-23, miR-378, or miR-505 enhances PRRSV infection. (A, B, and C) PAMs were transfected with inhibitors of the three indicated miRNAs or negative control miRNA (NC-inhib) for 24 h, and then infected with JXwn06 (MOI = 0.01). Thirty-six hour later, cells were fixed for detection of PRRSV N protein by immunofluorescent staining (A), or harvested for the analysis of ORF7 expression using qRT-PCR, normalized to GAPDH (B). Culture supernatants were collected for virus titer analysis (C). (D) qRT-PCR analysis of expression of endogenous miRNAs in PAMs. U6 was used as a control. CT, cycle threshold. Data were representative of three independent experiments (mean ± SD). Statistical significance was analyzed by *t*-test; $^{*}P < 0.05$.

miRNAs can positively modulate immune responses to generate a less permissive environment for viral replications (Wang et al., 2010a). Recently, more and more miRNAs have been reported to be involved in the regulation of immune systems including cytokine responses, as well as intracellular signaling pathways (Contreras and Rao, 2012; Olivieri et al., 2013). Whether host immune-related miRNAs could affect PRRSV infection has not been investigated.

The immune system initially recognizes virus infection and evokes antiviral responses by producing type I interferons (IFNs), which are essential for both innate and adaptive immunity. Different ligands can bind to Toll-like receptors (TLRs) and RIG-I-like receptors (RLRs) and recruit kinases that mediate the activation of the transcription factors AP-1 (heterodimer of ATF2 and c-Jun), NF-κB, IRF3 and IRF7, which are all required for initiating the production of IFN-α/β (Baccala et al., 2007). Type I interferons can initiate the activation of JAK/STAT signaling to induce hundreds of IFN-stimulated genes (ISGs), which play an important role in antiviral activities (Katze et al., 2002). Lots of miRNAs have been characterized in regulating IFN production (Contreras and Rao, 2012; Zhang et al., 2012; Zhou et al., 2010) and maintaining mRNA stability (Li et al., 2012; Witwer et al., 2010), as well as in regulating IFN downstream signals to modulate antiviral immunity (Papadopoulou et al., 2012; Yoshikawa et al., 2012). Most of them are identified to down-regulate the production of IFNs (Alam and O'Neill, 2011), whereas few miRNAs suggesting a positive role in induction of type I IFNs have been reported.

Our previous study identified that mir-181 could suppress PRRSV infection both *in vitro* and *in vivo* by directly targeting PRRSV genome and down-regulating CD163, a vital receptor of PRRSV (Gao et al., 2013; Guo et al., 2013). In order to find more potent PRRSV inhibitors, we screened potential miRNAs against PRRSV infection through ectopic expression of 12 candidate miRNAs and demonstrated that miR-23, miR-505, and miR-378 effectively suppressed PRRSV replication by directly targeting viral RNAs. Moreover, miR-23 increased the expression of type I interferons during PRRSV infection by enhancing IRF3/IRF7 signaling, which might further inhibit PRRSV replication. Our study here defined three host miRNAs antagonizing PRRSV, suggesting that miR-23, miR-378, and miR-505, in particular miR-23, could be used as antiviral therapy against PRRSV infection.

Results

miR-23, miR-378, and miR-505 inhibit PRRSV replication

Through miRNA target site (TS) prediction and conservation analysis on genomic RNAs of 168 type 2 PRRSV strains (Table 1) using RegRNA (Huang et al., 2006) or ViTa (Hsu et al., 2007) as described before (Guo et al., 2013), we selected 12 miRNAs including miR-23, miR-505, miR-378, mir-106, mir-128, mir-107, mir-34, mir-146, mir-15, mir-16, mir-223, and mir-101 as candidate miRNAs for PRRSV inhibition analysis as their target sites

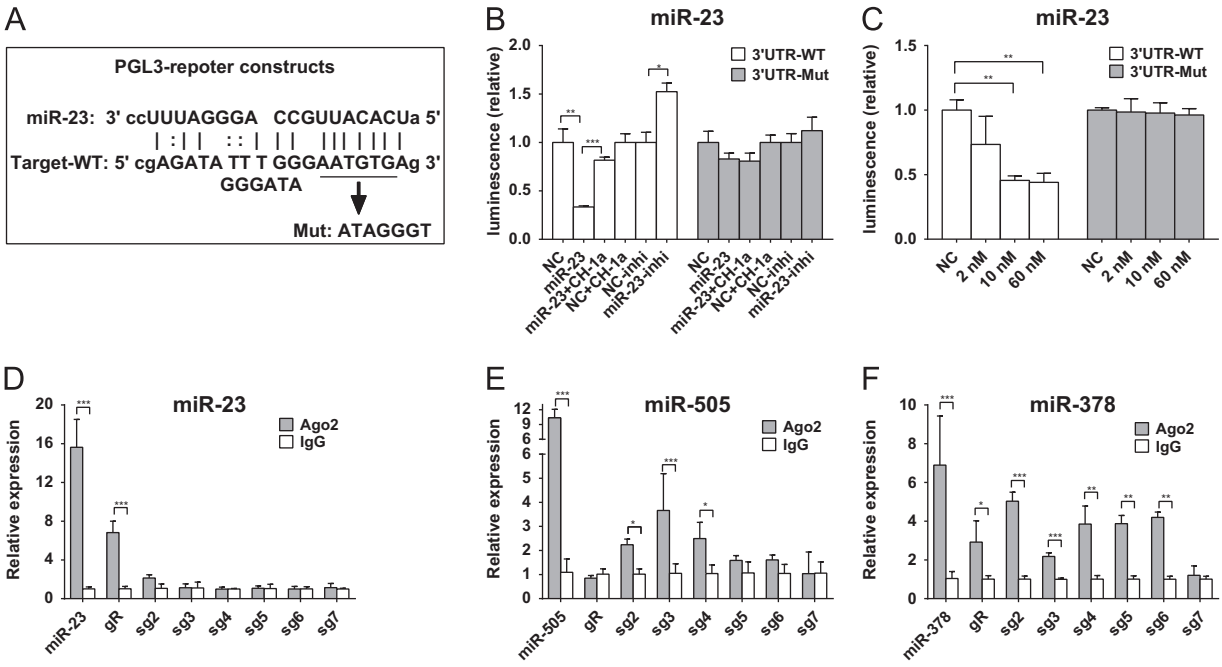

Fig. 4. miR-23, miR-378, and miR-505 directly target PRRSV genomic RNA and subgenomic RNAs. (A, B, and C) miR-23 directly targets PRRSV genomic RNA. (A) Diagram of the predicted target site for miR-23 in PRRSV genomic RNA. Seed sequences of miR-23 were underlined and mutated as indicated by the arrow. (B and C) Marc-145 cells were infected with or without CH-1a at an MOI of 0.1 for 2 h, then co-transfected with wt or mutant luciferase reporter vectors, pRL-TK and miR-23 mimics or inhibitor (B) or with different concentrations of miR-23 mimics (C). Cells in (B) and (C) were lysed 30 h post-transfection for dual-luciferase assay. (D, E, and F) miR-23, miR-378, and miR-505 physically bind to viral genomic and subgenomic RNAs in the RISC. qRT-PCR analysis of the relative expression of subgenomic mRNAs (sgRNAs), genomic RNA (gRNA), and the indicated miRNAs in the total RNA extracted from RISC-IP samples from PAMs transfected with miR-23 (D), miR-505 (E) or miR-378 (F) mimics subsequently infected with PRRSV JXwn06 at an MOI of 0.01, normalized to GAPDH. Data were representative of three independent experiments (mean ± SD). Statistical significance was analyzed by *t*-test; $^{*}P < 0.05$; $^{**}P < 0.01$; $^{***}P < 0.001$.

were well conserved in type 2 PRRSV strains (Table 1). Of them, the target sites of miR-23, miR-378, and miR-505 were highly conserved (98.13%, 96.84%, and 95.00%, respectively) in type 2 PRRSV strains.

To examine whether these miRNAs can inhibit PRRSV, we transfected each of the 12 miRNAs mimics into PAMs and tested their effects on PRRSV replication. Our results showed that among the 12 miRNA candidates, miR-23, miR-505, and miR-378 significantly impaired JXwn06 strain replication, reducing the virus yields about 10, 10, and 5 folds lower relative to NC, respectively (Fig. 1A and B). To rule out the possibility that transfection of miRNA mimics could affect PAM viability to affect PRRSV infection, MTT assay was performed after transfection of each of the 12 miRNAs mimics into PAMs. Our results showed that transfection of the mimics had no effects on cell viability (Fig. 1C). A previous study had suggested a role of the miR∼23a∼27a∼24-2 cluster in inducing apoptosis (Chhabra et al., 2009). In order to clarify whether miR-23 alone could induce apoptosis to affect the replication of PRRSV, we performed a TUNEL assay after transfection of miR-23 mimics. Our results showed that over-expression of miR-23 did not induce significant apoptosis compared with NC (Fig. 1D).

To further confirm these results, we transfected mir-23, mir-505, or mir-378 mimics at different doses into PAMs, and our results showed that both mRNA levels of ORF7 and virus titers were significantly decreased in a dose-dependent manner (Fig. 2A and B). Transfection of miR-23, miR-505, or miR-378 mimics at the concentration of 60 nM could induce a 94%, 84%, and 80% decrease of the PRRSV (JXwn06) ORF7 gene expression relative to NC in PAMs, respectively (Fig. 2A), resulting in a significant suppression of infectious viral particle production (∼30-, 10-, and 5-fold decrease, respectively) (Fig. 2B). The inhibitory effect was also confirmed by Western blot and the level of PRRSV GP5 was reduced dose-dependently (Fig. 2C). Notably, the inhibitory property of the three miRNAs was not restricted to JXwn06 strain, as a similar suppression was observed on traditional PRRSV strain CH-1a (Fig. 2A and B). We showed that when the cells were transfected with miRNA mimics at a concentration of 60 nM, the viability of PAMs was not affected. Thus, the dose (60 nM) was used in the following experiment.

To further verify whether these three miRNAs target PRRSV RNA and serve as direct antiviral factors, we infected PAMs with PPRSV following the transfection of the corresponding miRNA inhibitors and examined their effects on PRRSV replication. As expected, blockage of the endogenously expressed host miR-23, miR-505, or miR-378 significantly enhanced PRRSV infection compared to NC (Fig. 3A, B, and C), and the increase of viral yields was about 5, 2, and 3 folds for miR-23, miR-505, and miR-378, respectively (Fig. 3C). Among the three miRNAs, inhibition of miR-23 had the most effective effect, which might be due to its highest expression level in PAMs (Fig. 3D). Taken together, these data suggested that among the 12 candidate miRNAs, miR-23, miR-378, and miR-505 have the potential to inhibit PRRSV infection.

miR-23, miR-505, and miR-378 suppress PRRSV infection through directly binding to PRRSV genomic and subgenomic RNAs

To investigate whether the reduced viral yields are due to the direct targeting by these three miRNAs, we constructed firefly luciferase reporter pGL3-3′UTR-WT containing the predicted target site in the 3′ UTR, and another construct pGL3-3′UTR-Mut with mutations in the seed region (Fig. 4A) (Since our data in Fig. 2 suggested that miR-23 was the most effective one of the three miRNAs in PRRSV inhibition, we here used miR-23 as an example). In the presence of miR-23, the luciferase activity of 3′UTR-WT was significantly impaired to 33% relative to NC, which was rescued by

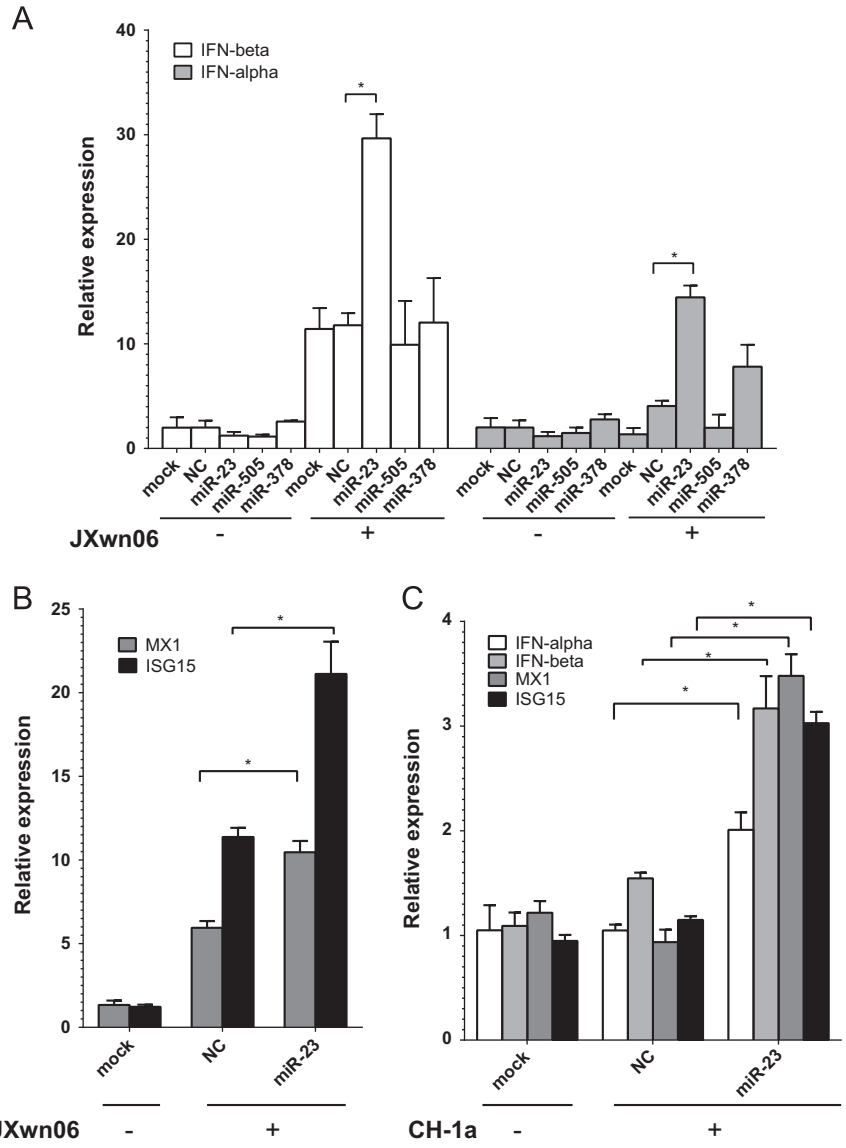

Fig. 5. miR-23 increases type I IFN expression during PRRSV infection. qRT-PCR analysis of the expression of type I IFNα/β (A and C) and IFN-stimulated genes (MX1, ISG15) (B and C) in PAMs transfected with the indicated miRNAs mimics or left un-treated (mock) for 24 h, and then infected with either JXwn06 (A and B) or CH-1a (C) for 48 h at an MOI of 0.01, or left untreated. The data were normalized to GAPDH and were representative of three independent experiments (mean ± SD). Statistical significance was analyzed by *t*-test; $^{*}P < 0.05$.

mutating the six seed nucleotides of TS (3′UTR-Mut), or by CH-1a infection, in which virus RNAs might act as a sponge to attract free miR-23 (Fig. 4B). The endogenous miR-23 also played a role in inhibition, as blockage of miR-23 expression showed a ~1.5-fold increase in luciferase activity of 3′UTR-WT (Fig. 4B). Over-expression of miR-23 remarkably inhibited the luciferase activity of the 3′UTR-WT in a dose-dependent manner, with a highest inhibition percentage of 66% at 60 nM, while luciferase activity of 3′UTR-Mut was not affected (Fig. 4C). These results confirmed that the PRRSV genomic RNA harbored functional miR-23TS that was sufficient to confer miR-23-mediated repression of PRRSV infection.

For PRRSV, its transcription strategy involves the synthesis of a full-length genomic RNA and at least 6 nested subgenomic RNAs, which share partial common sequences. To test whether miR-23, miR-378, or miR-505 physically binds to the genomic and subgenomic RNAs (sg) to mediate the degradation of PRRSV RNAs, we performed the RISC-IP assay. miR-23 has a binding site on PRRSV ORF3 and might bind to genomic RNA and subgenomic RNA 2 (sg2). As expected, when miR-23 was over-expressed during PRRSV infection, we detected a ~16-fold enrichment of miR-23 and ~7-fold enrichment of viral genomic RNA on RISC compared to the IgG isotype control (Fig. 4D). However, the enrichment of sg2 on RISC was not significant, which might be due to other factors that influence the specificity of the miR-23. In the case of miR-505, it has TSs in ORF3 and ORF5, and three subgenomic RNAs (sg2, sg3, and sg4) were enriched 2 to 4 folds on RISC along with an over 10-fold enrichment of miR-505 (Fig. 4E). Over-expression of miR-378 increased its own load on RISC about 7-fold and enriched all viral RNAs 2 to 5 folds except for sg7 (Fig. 4F). Taken together, these data demonstrated that miR-23, miR-378, and miR-505 suppressed PRRSV replication by directly targeting its genomic and subgenomic RNAs.

miR-23 increases type I interferon expression during PRRSV infection.

miR-23 showed better inhibitory effects on PRRSV replication while its TS was not superior to the TS of miR-505 or miR-378, implicating that other mechanism might exist for miR-23 to suppress

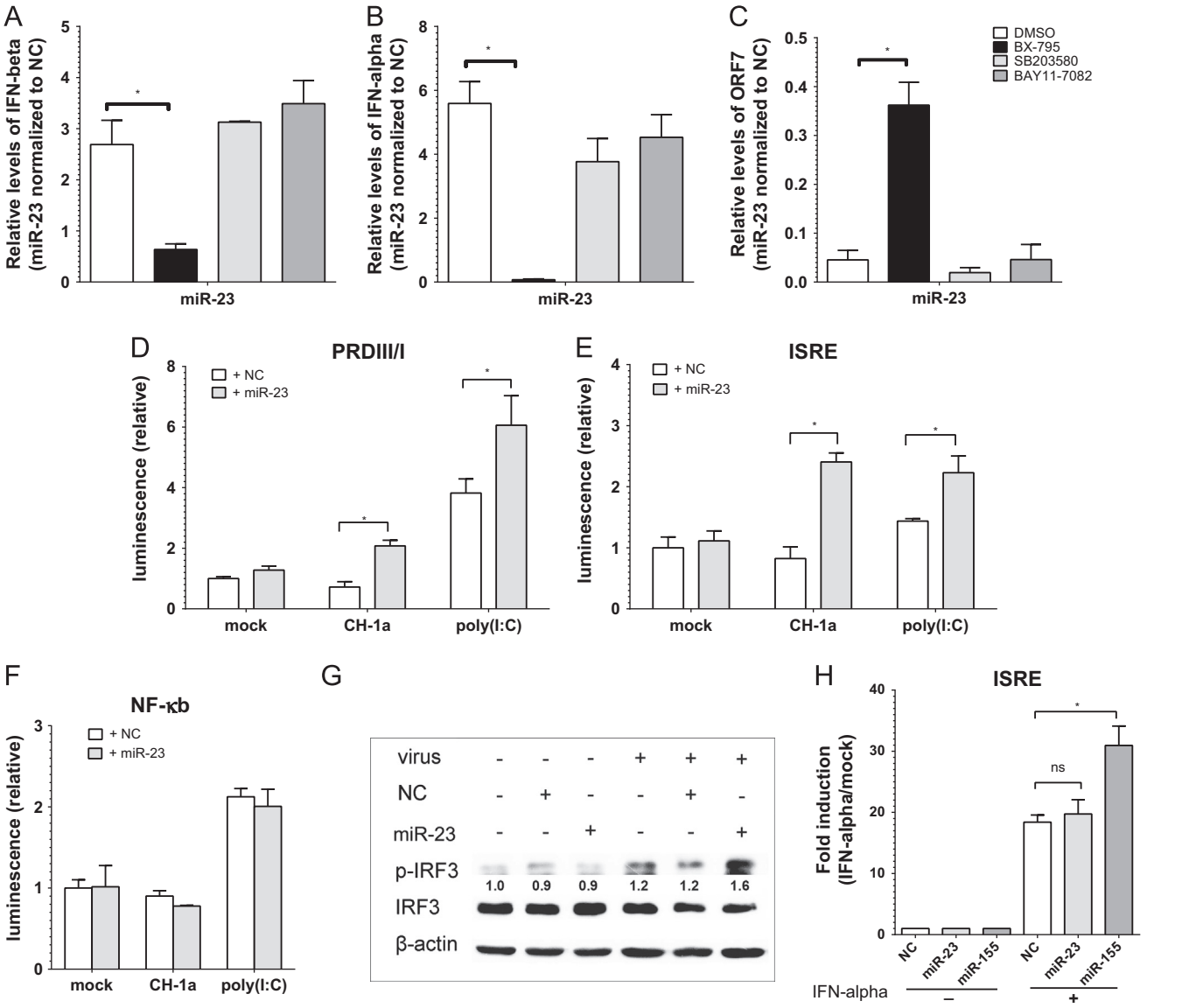

Fig. 6. miR-23 increases type I interferon expression through IRF3/IRF7 activation during PRRSV infection. (A, B and C) IRF3/IRF7 inhibitor impaired the induction of type I IFNs during PRRSV infection. Transfection of miR-23 mimics or NC in PAMs was performed prior to the treatment of the indicated inhibitors or DMSO, followed by PRRSV JXwn06 infection for 48 h (MOI=0.01). Cells were then harvested for quantifying the expression of type I interferon genes IFN-β (A) and IFN-α (B), and ORF7 (C) using qRT-PCR, normalized to GAPDH. The data were represented as fold changes of the indicated genes after over-expression of miR-23 (NC was set up as 1 and not shown in the figure). Statistical significance was analyzed by one-way ANOVA followed by post hoc Dunnett's multiple comparison. Significance compared to DMSO-baseline: $^{*}P<0.05$. (D, E, F, and G) miR-23 increases activation of IRF3 during PRRSV infection. Either miR-23 or NC mimics and pRL-TK were co-transfected with IRF3 (D), ISRE (E), or NF-κB (F) luciferase reporters into Marc-145 cells. Cells were then either infected with CH-1a (MOI=0.01) 6 h after transfection, or transfected with 1 μg poly(I:C) 24 h post trasfection, or left untreated (mock). All cells were harvested 36 h post-transfection for dual-luciferase assay. (G) Western blot analysis of phospho-IRF3 or IRF3 in PAMs transfected with miR-23 mimics followed by infection with JXwn06 (MOI=0.01) for 48 h. β-actin was shown as a loading control. (H) miR-23 plays no role in IFN downstream pathway. Luciferase activity in lysates of CRL-2843 cells co-transfected with ISRE luciferase reporter, pRL-TK and miRNA mimics for 6 h and incubated with or without 10 U/ml IFN-α for 24 h. The data were represented as fold increase of ISRE. Data were representative of three independent experiments (mean ± SD). Statistical significance was analyzed by *t*-test; $^{*}P<0.05$; ns, not significant.

PRRSV replication. Interestingly, we found that over-expression of miR-23 rendered the cells more competent in IFN-α and IFN-β expression during both JXwn06 (~3-fold higher) and CH-1a (~2-fold higher) infection when compared with NC (Fig. 5A and C). Moreover, the IFN-stimulated genes MX1 and ISG15 were also significantly up-regulated (Fig. 5B and C). However, over-expression of miR-505 or miR-378 did not increase type I IFN expression (Fig. 5A). To rule out the possibility that miRNAs themselves could serve as ligands for TLRs and activate IFNs (Fabbri et al., 2012; Lehmann et al., 2012), we delivered miRNA mimics into PAMs without PRRSV infection and quantitative real-time PCR was performed to detect IFNs expression. Our results showed that miR-23 did not mediate the activation of IFNs in the absence of PRRSV infection (Fig. 5A).

miR-23 increases the expression of type I interferons by the activation of IRF3/IRF7 during PRRSV infection

To gain insight into the underlying mechanisms of IFN induction by miR-23 during PRRSV infection, inhibitors of AP-1 (SB203580), NF-κB (BAY11-7082), IRF3 and IRF7 (BX-795) were applied. Quantitative PCR analysis of IFN-α/β expression showed that the ability of miR-23 to induce type I interferons was severely compromised when pretreated with IRF3/IRF7 inhibitor (Fig. 6A

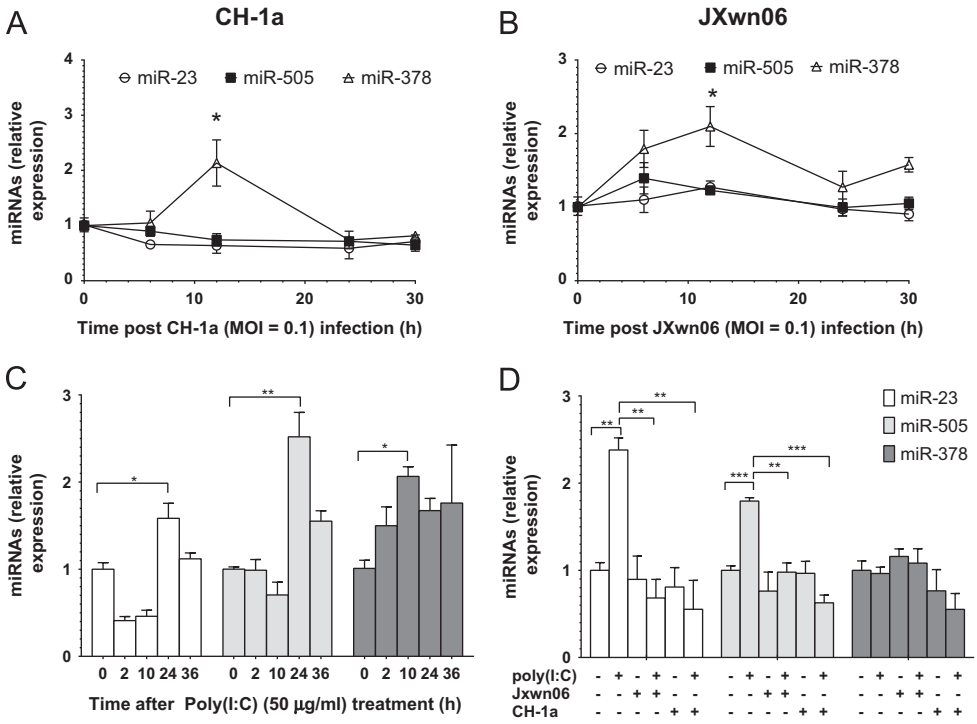

Fig. 7. PRRSV infection inhibits the poly(I:C)-induced miR-23 and miR-505. qRT-PCR analysis of miR-23, miR-378, and miR-505 in PAMs infected with JXwn06 (A) or CH-1a (B) at an MOI of 0.1, or incubated with 50 μg/ml poly(I:C) (C) for indicated times, or treated with 50 μg/ml poly(I:C) and simultaneously infected with PRRSV (MOI = 0.1) for 24 h (D). All the data were normalized to U6 and were representative of three independent experiments (mean ± SD). Statistical significance was analyzed by *t*-test; $^{*}P < 0.05$; $^{**}P < 0.01$; $^{***}P < 0.001$.

and B), suggesting that miR-23 mediates activation of type I IFNs during PRRSV infection through IRF3/IRF7 pathway. Importantly, interrupting the induced production of IFNs using IRF3/IRF7 inhibitor impaired the ability of miR-23 to inhibit PRRSV infection (from 20-fold reduction to 3-fold reduction) (Fig. 6C), suggesting that miR-23-induced IFNs might further inhibit PRRSV infection. To verify whether the IRF signals were up-regulated by miR-23, we made a reporter construct containing PRDIII/I regulatory element to monitor IRF activities. IRF activity was significantly increased to 2.9 folds in the presence of miR-23 when infected with CH-1a (Fig. 6D). We also used a reporter construct containing interferon-sensitive responsive element (ISRE) to monitor the downstream signals of IFNs. As expected, the ISRE response was also enhanced 2.9 folds by miR-23 during CH-1a infection (Fig. 6E). Interestingly, upon transfection of poly(I:C), a RIG-I-like receptors (RLRs) ligand into Marc-145 cells, the activity of IRFs and the response of ISRE were also increased about 2 folds by miR-23 (Fig. 6D and E), suggesting that miR-23 has the ability to induce IFN production in RLRs-mediated pathway. NF-κB did not participate in this pathway. Thus, we set up NF-κB reporter as a negative control. As expected, the activity of NF-κB was not altered by miR-23 (Fig. 6F). To further confirm the above results, we performed Western blot to detect the activated IRF3 (phospho-IRF3) signals. Consistent with our expectation, IRF3 activation was increased by miR-23 during PRRSV infection (Fig. 6G).

To investigate whether miR-23 could act on the IFN downstream pathway, we applied our experiments on CRL-2843 cells, which are derived from porcine alveolar macrophage and can respond well to porcine IFNs. We transfected CRL-2843 cells with ISRE-reporter vector and miR-23 or miR-155 mimics (as a positive control), and 6 h later, cells were mock treated or incubated with IFN-α. The induction folds of ISRE stimulated by IFN-α were calculated, which could represent the activation state of JAK/STAT signals. Using this assay, we confirmed that miR-23 did not significantly augment IFN-α-induced ISRE activity, suggesting that miR-23 was not involved in IFN-α downstream pathway (Fig. 6H). A previously study has shown that miR-155 was able to increase the JAK/STAT signals by inhibiting SOCS1 (Wang et al., 2010a). And as expected, miR-155 induced a more robust activation of JAK/STAT signals compared to NC (1.7 fold higher) (Fig. 6H).

Collectively, we showed here that IRF3/IRF7 played a critical role in miR-23-mediated induction of IFNs during PRRSV infection.

PRRSV infection does not induce the production of miR-23 and miR-505, but suppresses the poly(I:C)-induced miR-23 and miR-505 expression

To assess whether PRRSV influence the expression of miR-23, miR-378, and miR-505 to facilitate its infection, a time course analysis upon PRRSV infection was performed. Our results showed that miR-378 was induced to about 2- fold higher at 10 h post infection by both JXwn06 and CH-1a, while miR-23 and miR-505 remained stable (Fig. 7A and B). We then asked whether the three miRNAs could be regulated in antiviral innate immunity against RNA virus. We found that upon poly(I:C) incubation, which mimics virus dsRNA stimulation, miR-23 and miR-505 were induced about 1.6-, and 2.5- folds at 24 h, respectively, and miR-378 was increased about 2.1 folds at 10 h (Fig. 7C). Interestingly, our results showed that PRRSV suppressed poly(I:C)-induced miR-23 and miR-505 expressions at 24 h (Fig. 7D), which might be a strategy for PRRSV to evade the RNA-mediated immune response induced in TLR3 pathway.

Discussion

miRNAs are emerging as active and versatile regulators of immune response and intricate networks of host-pathogen interactions. Herein, we identified miR-23, miR-378, and miR-505 as important inhibitors of the PRRSV replication by directly targeting

Table 2
Sequences of mimics and inhibitors of 12 miRNAs used in screening for anti-PRRSV miRNAs.

miRNAs	Mimics sequence (5′→3′)	Inhibitor sequence (5′→3′)
miR-23	AUCACAUUGCCAGGGAUUUCC	GGAAAUCCCUGGCAAUGUGAU
miR-505	UCAACACUUGCUGGUUUCCUCU	AGAGGAAACCAGCAAGUGUUGA
miR-378	ACUGGACUUGGAGUCAGAAGGC	GCCUUCUGACUCCAAGUCCAGU
miR-106	AAAAGUGCUUACAGUGCAGGUAGC	
miR-128	UCACAGUGAACCGGUCUCUUU	
miR-107	AGCAGCAUUGUACAGGGCUAUCA	
miR-34	UGGCAGUGUCUUAGCUGGUUGU	
miR-146	UGAGAACUGAAUUCCAUAGGC	
miR-15	UAGCAGCACAUAAUGGUUUGU	
miR-16	UAGCAGCACGUAAAUAUUGGCG	
miR-223	UGUCAGUUUGUCAAAUACC	
miR-101	UACAGUACUGUGAUAACUGAA	

Table 3
Primers and sequences used in RT-PCR and cloning.

Primers	Sequence (5′→3′)
U6-F	CTCGCTTCGGCAGCACA
U6-R	AACGCTTCACGAATTTGCGT
ORF7-F	AATAACAACGGCAAGCAGCA
ORF7-R	GCACAGTATGATGCGTCGGC
GAPDH-F	CCTTCCGTGTCCCTACTGCCAAC
GAPDH-R	GACGCCTGCTTCACCACCTTCT
MX1-F	CACAGAACTGCCAAGTCCAA
MX1-R	GCAGTACACGATCTGCTCCA
ISG15-F	GGTGCAAAGCTTCAGAGACC
ISG15-R	GTCAGCCAGACCTCATAGGC
IFN-beta-F	AGCACTGGCTGGAATGAAAC
IFN-beta-R	TCCAGGATTGTCTCCAGGTC
IFN-alpha-F	CTGCTGCCTGGAATGAGAGCC
IFN-alpha-R	TGACACAGGCTTCCAGGTCCC
miR-23-F	CGATCACATTGCCAGGGATTTCC
miR-378-F	ACTGGACTTGGAGTCAGAAGGC
miR-505-F	GCTCAACACTTGCTGGTTTCCTCT
Uni-miR-R primer	GCGAGCACAGAATTAATACGACTCAC
3′UTRwt-F	GACTCTAGAATGAAATGGGGTCTATGCA
3′UTRwt-R	GACTCTAGAGTGTTGGTAGTAGGTCTG
3′UTRmut-F	CGGCCCAGTTCCATCCCGAGATATTTGGGATAGGGTACATACGTC
3′UTRmut-R	TGGTGCTTGATGTCAACATAAACTTGACGTATGTACCCTATCCCA
NF-κB responding element	GTGGGAAATTCCGTGGGAAATTCCGTGGGAAATTCCGTGGGAAATTCC
ISRE responding element	TCGAGAAACTGAAACTGAAACTGAAACTGAAACTGAAACTGAAACTGAAACTGAAACT
IRFs responding element (PRDIII/I)	TCGAGAAAACTGAAAGGGAGAACTGAAAGTGAAAACTGAAAGGGAGAACTGAAAGTGAAAACTGAAAGGGAGAACTGAAAGTG

PRRSV genomic and subgenomic RNAs. Moreover, mir-23 was also shown to increase type I IFN expression and possibly generate a less permissive environment for PRRSV replication.

Multiple lines of evidence have confirmed that miRNAs can modulate RNA-mediated host defenses against viral infection through two mechanisms. First, miRNAs can serve a direct antiviral function through viral RNA binding. As for the primate foamy virus PFV) (Lecellier et al., 2005), host miR-32 targets the viral genome to efficiently restrain viral replication. Five interferon (IFN)-induced miRNAs (mir-196, mir-296, mir-351, mir-431 and mir-448) are shown to target the HCV genome and can inhibit HCV replication (Pedersen et al., 2007). Second, miRNAs can indirectly modulate host factors to provide a less permissive environment for virus replication. For example, the miRNA cluster mir-17/92 was found to be a negative regulator of HIV through inhibiting cellular factor PCAF, which is important for efficient HIV replication (Triboulet et al., 2007). Similar to these results, we show here that miR-23 inhibits PRRSV replication by directly targeting PRRSV RNAs and that it may also inhibit PRRSV replication indirectly by up-regulating type I interferons.

We showed that miR-23, miR-378, and miR-505 were antiviral host factors against PRRSV (Fig. 1), and the three miRNAs could significantly reduce the replication of both JXwn06 and CH-1a strains (Fig. 2). From miRNA target site prediction and conservation analysis (Table 1), we showed that the target sites of miR-23, miR-505, and miR-378 were highly conserved among type 2 PRRSV isolates. Moreover, blockage of endogenous miR-23, miR-378, and miR-505 significantly increased PRRSV infection (Fig. 3). Our data suggested that miR-23, miR-378, and miR-505 may play a role in the cellular responses to PRRSV infection.

PRRSV synthesizes a full-length genomic RNA and at least 6 nested subgenomic RNAs, which share partial common sequences. Thus, we proposed that besides genomic RNA, an miRNA might target other corresponding subgenomic RNAs containing its TSs, which might imply a more robust RNA-mediated defense against PPRSV as sequence-specific binding sites increase. The results of RISC-IP supported our expectation (Fig. 4). We showed that almost all subgenomic RNAs harboring TSs were enriched in RISC along with corresponding miRNAs. Therefore, our data demonstrated that miR-23, miR-378, and miR-505 were novel antiviral host factors against PRRSV by directly binding to the genomic or subgenomic RNAs.

In addition, we demonstrated that miR-23 induced type I IFN expression through activation of IRF3/IRF7 (Figs. 5 and 6), which might further inhibit PRRSV infection. To our knowledge, this is the first

report about a miRNA-mediated activation of type I IFNs during viral infection. Various kinds of strategies are taken by viruses to inhibit IFN system. PRRSV exhibits significant inhibition of type I IFN production in both virus-infected cells and pigs by encoding IFN antagonists, which include at least three non-structural proteins (Nsp1, Nsp2, and Nsp11) and a structural protein (N protein) (Sun et al., 2012). The induction of IFNs by miR-23 was not due to the low expressed IFN antagonists, because in the case of miR-505, it was unable to induce IFNs, even though they both exhibited comparable inhibition of PRRSV (Fig. 5A). But the possibility that miR-23 interfered with certain PRRSV proteins that may disturb IRF3/IRF7 activation could not be excluded. To investigate the exact target factors of miR-23, we tested some host candidates predicted to be targeted by miR-23, which have been shown to negatively regulate IRF3/IRF7, including A20 (Parvatiyar et al., 2010) and TAX1BP1 (Parvatiyar et al., 2010; Verstrepen et al., 2011). However, RISC-IP results showed that they were not authentic targets of miR-23 (data not shown). Over one thousand conserved target mRNAs of miR-23 were predicted by Targetscan, including a large scale of un-characterized proteins, among which might exist one or more miR-23 target(s) involved in negative regulation of IRF3/IRF7 during PRRSV infection. This needs to be investigated in the future. IRF3/IRF7 are pivotal transcription factors of type I IFNs that participate in all pathogen recognition receptors (PRRs) signaling pathways initiating innate immunity. Our data suggested an augmentation of IRF signals mediated by miR-23 through RLR signaling pathways (Fig. 6D), implicating that miR-23 might play a role in regulation of pathogen-host interaction and in innate immunity.

miRNA biogenesis is a highly regulated process in eukaryotic cells. mir-23 was induced by poly(I:C) (Fig. 7C), a TLR3 ligand, which might contribute to virus inhibition achieved by poly(I:C) (Zhang et al., 2013a, 2013b). Multiple strategies have been employed by PRRSV to counteract TLR and RLR-mediated antiviral activities. As previously shown, mir-23 was induced by NF-κB (Zhou et al., 2009). And it has been demonstrated that NF-κB was delayed in activation during PRRSV infection until 36–48 hpi (Lee and Kleiboeker, 2005). Thus, we proposed that the delayed induction of NF-κB during PRRSV infection might inhibit or impair the induction of mir-23 by NF-κB to facilitate its infection. Interestingly, we found that PRRSV suppressed the poly (I:C)-induced mir-23 expression (Fig. 7D).

Overall, we demonstrated that over-expression of miR-23, miR-378, and miR-505 could inhibit PRRSV replication. Additionally, although clearly defining the physiological role of miR-23 remains an unfinished task, our study provided evidence that miR-23 enhanced type I IFN expression during PRRSV infection, suggesting that miR-23 could be used as an antiviral therapy against PRRSV infection.

Materials and methods

Cells and viruses

Marc-145 cells, a monkey kidney cell line highly permissive for PRRSV infection, were maintained in DMEM supplemented with 10% fetal bovine serum (FBS) and penicillin/streptomycin and were purchased from the American Type Culture Collection (ATCC no. CRL-1223). CRL-2843 cells (ATCC no. CRL-2843), which are a porcine alveolar macrophage cell line, were maintained in RPMI 1640 medium supplemented with 10% FBS and penicillin/streptomycin. Porcine alveolar macrophages (PAMs) were obtained by lavaging lungs of 8-week-old specific-pathogen-free (SPF) pigs and maintained as CRL-2843 cells.

Two type 2 PRRSV strains were used: one was CH-1a (the first type 2 PRRSV strain isolated in China; GenBank accession, AY032626), which was propagated and titrated in Marc-145 cells; and the other one was JXwn06 (a strain isolated from a pig farm with an atypical PRRS outbreak in Jiangxi province, China in 2006; GenBank accession, EF641008.1), which was propagated and titrated in PAMs. Briefly, PRRS virus was serially diluted 10-fold in complete RPMI 1640 to infect 5×10^4 PAMs in 96-well plates. PRRSV infection was determined 72 h post infection using immunofluorescent staining for PRRSV N protein. Titrated viruses were then stored at −80 °C until use.

Reagents

Recombinant swine IFN-α was kindly provided by Dr. Wenjun Liu (Chinese Academy of Sciences, Beijing, China). All miRNA mimics and inhibitors listed in Table 2 were synthesized from GenePharma (Shanghai, China). NF-κB inhibitor (BAY11-7082) and MAPK (p38) inhibitor (SB203580) were purchased from Enzo Life Sciences. TBK1 inhibitor (BX-795) was purchased from Selleck Chemicals.

Transfection of miRNA mimics or inhibitors

PAMs or Marc-145 cells were seeded in 12-well plates for 12 h, and then mimics or inhibitors of miRNAs (60 nM, except for the dose-dependent experiments) were transfected using Hiperfect transfection reagents (Qiagen). Twenty-four hours after transfection, cells were infected with PRRSV. Thirty-six or forty-eight hours later, the supernatant was collected for virus titration and cells were fixed for indirect immunofluorescent staining or collected for RNA quantification or Western blot analysis.

RNA isolation and quantitative real-time PCR (qRT-PCR)

Cells were harvested using Trizol (Invitrogen) reagent and RNA was extracted following the manufacturer's protocol. For miRNAs, poly(T) adapter RT-PCR was applied as previously described (Shi et al., 2012). U6 RNA was set up as an endogenous control. miRNAs or mRNAs were reverse transcribed with M-MLV Reverse Transcriptase (Takara) and amplified by using FastSYBR Mixture (Cwbiotech) on a ViiA™ 7 real-time PCR System (Applied Biosystems). Specific primers for quantitative analysis of the mRNAs were designed and listed in Table 3. Primers used to detect genomic and subgenomic RNAs were used as previously described (Guo et al., 2013). GAPDH was set up as endogenous controls. All quantitative real-time PCR experiments were done in triplicate.

Immunofluorescence assay

For detection of PRRSV infection in PAMs, immunofluorescence assay (IFA) was performed. Cells were fixed in cold methanol-acetone (1:1) for 10 min at 4 °C, washed with phosphate-buffered saline (PBS), and then blocked with 10% goat serum in PBS for 30 min. After blocking, cells were incubated with anti-PRRSV nucleocapsid protein monoclonal antibody SNOW17 (1:10,000; Rural Technologies), or an isotype control antibody for 60 min at room temperature. After washing, cells were then incubated with FITC-conjugated goat anti-mouse IgG antibody (1:2000, Jackson ImmunoResearch) for 1 h at 37 °C. Cells were then examined using fluorescence microscopy.

Western blot

For detection of PRRSV structural protein GP5 and host Phospho-IRF3, and IRF3 proteins, cells were lysed with RIPA with a protease cocktail and proteins were separated on 12% SDS-PAGE gels and transferred onto polyvinylidene fluoride (PVDF) membranes. Membranes were blocked with 5% milk in PBS with Tween-20 (PBST 0.025% Tween-20) and probed with Rabbit anti-GP5 polyclonal antibodies (1:5000, prepared in our lab),

anti-Phospho-IRF3 polyclonal antibodies (1:1000; #4947, Cell Signaling), or anti-IRF3 polyclonal antibodies (1:1000; #119041, Cell Signaling) for 1 h at room temperature. HRP-conjugated anti-Rabbit secondary antibodies (1:5000, Santa Cruz Biotechnology) were used to detect primary antibodies, and proteins were visualized by chemiluminescence. β-actin (1:5000, Sigma) was set up as a loading control. The intensity of phospho-IRF3 and β-actin were quantified using Quantity One software (Bio-Rad) and the relative gray level of phospho-IRF3 over β-actin was used to represent the signal strength for phospho-IRF3.

RISC immunoprecipitation (RISC-IP) assay

For confirming the physical interaction between miRNAs and target RNAs, RISC-IP assay was performed. We adapted the protocol described previously (Wang et al., 2010b) for immunoprecipitating Argonaute-2 (Ago2)-mRNA complexes. Briefly, PAMs were seeded in six-well plates and infected with JXwn06 (MOI=0.01) for 36 h following the transfection of miR-23, miR-505, or miR-378 mimics (60 nM) for 24 h. Then cells were lysed with RIPA with a protease cocktail. Cell lysates were cleared by centrifugation. Protein-G (40 μl, Abmart) was incubated with 5 μg of Ago2 antibody (H00027161-M01, Abnova) or an isotype control IgG (Beyotime). Beads-antibody complex was blocked with 500 μg/ml yeast RNA (Hualan Chem) for 30 min, followed by 3 washes with PBS and 2 washes with RIPA. Then cleared lysate was incubated with pre-treated antibody-protein-G beads overnight at 4 °C. Beads were washed 8 times with PBS and finally re-suspended in 250 μl RIPA. Ago2-RNA complexes were extracted by adding 750 μl of Trizol-LS reagent (Invitrogen) directly to the beads.

Construction of luciferase reporters and luciferase assays

In order to confirm the target site of miR-23, a 1024 bp fragment around the predicted miR-23 target site in the PRRSV strain JXwn06 genome was amplified and inserted downstream of the Firefly luciferase gene in the pGL3-control vector (Promega) at the XbaI site to create the wild type 3′UTR vector. miRNA seed site mutant was made by mutating the underlined 6 nucleotides in the 7-mer-m8 seed sequences (5′-cgAGATATTTGGGATAGGGAATGTGAg-3′ mutated to 5′-cgAGATATTTGGGATAGGGATAGGGTg-3′) using a site-directed mutagenesis kit (Stratagene) following the manufacture′s instructions. For monitoring the activities of transcription factors, NF-κB, ISRE, and IRF3 responding elements were synthesized and annealed to form double-stand DNA, and then separately cloned into pGL3-basic promoter region. Another vector pRL-TK containing the Renilla luciferase was used as a normalization control. All sequences mentioned above were shown in Table 3.

For luciferase reporter assay, Marc-145 or CRL-2843 cells were seeded in 12-well plates 12 h before transfection. For cotransfection, 400 ng Firefly luciferase and 20 ng Renilla luciferase reporter plasmids were transiently transfected into cells with miRNA mimics or inhibitors (60 nM, except for the dose-dependent experiments) using Lipofectamine 2000 (Invitrogen) for 30 h. In order to test the impact of miR-23 on RLR pathway, 24 h after the delivery of the mixture of luciferase reporter vectors and miR-23, transfection of poly(I:C) (1 μg) into Marc-145 cells was performed with Lipofectamine LTX Reagent (Invitrogen) to activate the RLR pathway for 12 h. And then, all the cells were harvested for luciferase activity assay using the Promega Dual Luciferase kit according to manufacturer′s instructions.

Inhibition of signal transduction pathways

Transfection of miR-23 mimics or NC (60 nM) into PAMs for 24 h was performed prior to the treatment with dimethyl sulfoxide (DMSO; 1 μM), NF-κB inhibitor BAY11-7082 (1 μM), p38 mitogen-activated protein kinase (MAPK) inhibitor SB203580 (5 μM), or TBK1 inhibitor BX-795 (1 μM). After 1 h incubation with the inhibitors, PAMs were infected with JXwn06 (MOI=0.01) in the presence of the inhibitors. Forty-eight hours later, cells were harvested for quantitative real-time PCR analysis.

MTT assay

The MTT [3-(4,5-dimethyl-2-thiazolyl)-2,5-diphenyl-2H-tetrazolium bromide] assay was used to examine the effect of transfection with the mimics on cell viability. PAMs in 96-well plates were transfected with 60 nM miRNAs for 72 h. And then, 20 μl of freshly made 5 mg/ml MTT solution was added to each well, and the cells were incubated for another 5 h at 37 °C before the medium was replaced with 200 μl DMSO to dissolve the crystals. The plates were further incubated at 37 °C for 5 min to dissolve any air bubbles before the MTT signal was measured at an absorbance of 550 nm.

TUNEL assay

Detection of cell apoptosis was performed using the TUNEL assay following the manufacturer′s protocol (Millipore). Briefly, cells were fixed with 1% paraformaldehyde in PBS for 10 min at room temperature. After rinsing with PBS, cells were permeabilized using 0.3% Triton X-100 in 0.1% sodium citrate for 4 min. Then, cells were incubated with the TdT (terminal deoxynucleotidyl transferase) enzyme for 1 h at 37 °C. After stopping the reaction with stop buffer, cells were washed with PBS and stained with the anti-digoxigenin-florescein for 30 min at 37 °C in the dark. After rinsing with PBS, cells were counterstained with DAPI. Stained cells were visualized using a fluorescence microscope. Six visual fields were randomly selected, and TUNEL-positive and DAPI positive cells were counted. Results were represented as percentage of TUNEL-positive cells relative to DAPI-positive cells.

Statistical analysis

Generally, experiments were performed with at least three independent experiments, with three technical replicates for each experiment (except for the Western and TUNEL experiments). Results were analyzed by GraphPad Prism (GraphPad Software, San Diego, *CA*) using *Student′s t*-test or ordinary one-way ANOVA followed by post hoc Dunnett′s multiple comparison. Differences were considered to be statistically significant if the *P* value is less than 0.05. $^{*}P<0.05$; $^{**}P<0.01$; $^{***}P<0.001$.

Acknowledgments

This work was supported by the Faculty Starting Grant and State Key Laboratory of Agrobiotechnology (Grant 2010SKLAB06-1 and 2012SKLAB01-6), China Agricultural University, China.

References

Alam, M.M., O'Neill, L.A., 2011. MicroRNAs and the resolution phase of inflammation in macrophages. Eur. J. Immunol. 41, 2482–2485.
Allende, R., Lewis, T.L., Lu, Z., Rock, D.L., Kutish, G.F., Ali, A., Doster, A.R., Osorio, F.A., 1999. North American and European porcine reproductive and respiratory syndrome viruses differ in non-structural protein coding regions. J. Gen. Virol. 80 (Pt 2), 307–315.
Baccala, R., Hoebe, K., Kono, D.H., Beutler, B., Theofilopoulos, A.N., 2007. TLR-dependent and TLR-independent pathways of type I interferon induction in systemic autoimmunity. Nat. Med. 13, 543–551.
Bartel, D.P., 2009. MicroRNAs: target recognition and regulatory functions. Cell 136, 215–233.

Carthew, R.W., Sontheimer, E.J., 2009. Origins and mechanisms of miRNAs and siRNAs. Cell 136, 642–655.
Cavanagh, D., 1997. Nidovirales: a new order comprising Coronaviridae and Arteriviridae. Arch. Virol. 142, 629–633.
Chhabra, R., Adlakha, Y.K., Hariharan, M., Scaria, V., Saini, N., 2009. Upregulation of miR-23a-27a-24-2 cluster induces caspase-dependent and -independent apoptosis in human embryonic kidney cells. PloS One 4, e5848.
Contreras, J., Rao, D.S., 2012. MicroRNAs in inflammation and immune responses. Leukemia 26, 404–413.
Fabbri, M., Paone, A., Calore, F., Galli, R., Gaudio, E., Santhanam, R., Lovat, F., Fadda, P., Mao, C., Nuovo, G.J., Zanesi, N., Crawford, M., Ozer, G.H., Wernicke, D., Alder, H., Caligiuri, M.A., Nana-Sinkam, P., Perrotti, D., Croce, C.M., 2012. MicroRNAs bind to Toll-like receptors to induce prometastatic inflammatory response. Proc. Natl. Acad. Sci. USA 109, E2110–2116.
Firth, A.E., Zevenhoven-Dobbe, J.C., Wills, N.M., Go, Y.Y., Balasuriya, U.B., Atkins, J.F., Snijder, E.J., Posthuma, C.C., 2011. Discovery of a small arterivirus gene that overlaps the GP5 coding sequence and is important for virus production. J. Gen. Virol. 92, 1097–1106.
Gao, L., Guo, X.K., Wang, L., Zhang, Q., Li, N., Chen, X.X., Wang, Y., Feng, W.H., 2013. MicroRNA-181 suppresses PRRSV infection by targeting its receptor CD163. J. Virol.
Gottwein, E., Mukherjee, N., Sachse, C., Frenzel, C., Majoros, W.H., Chi, J.T., Braich, R., Manoharan, M., Soutschek, J., Ohler, U., Cullen, B.R., 2007. A viral microRNA functions as an orthologue of cellular miR-155. Nature 450, 1096–1099.
Guo, X.K., Zhang, Q., Gao, L., Li, N., Chen, X.X., Feng, W.H., 2013. Increasing expression of microRNA 181 inhibits porcine reproductive and respiratory syndrome virus replication and has implications for controlling virus infection. J. Virol. 87, 1159–1171.
Hsu, P.W., Lin, L.Z., Hsu, S.D., Hsu, J.B., Huang, H.D., 2007. ViTa: prediction of host microRNAs targets on viruses. Nucleic Acids Res., 35; , pp. D381–385.
Huang, H.Y., Chien, C.H., Jen, K.H., Huang, H.D., 2006. RegRNA: an integrated web server for identifying regulatory RNA motifs and elements. Nucleic Acids Res. 34, W429–434.
Huang, J., Wang, F., Argyris, E., Chen, K., Liang, Z., Tian, H., Huang, W., Squires, K., Verlinghieri, G., Zhang, H., 2007. Cellular microRNAs contribute to HIV-1 latency in resting primary CD4+ T lymphocytes. Nat. Med. 13, 1241–1247.
Johnson, C.R., Griggs, T.F., Gnanandarajah, J., Murtaugh, M.P., 2011. Novel structural protein in porcine reproductive and respiratory syndrome virus encoded by an alternative ORF5 present in all arteriviruses. J. Gen. Virol. 92, 1107–1116.
Katze, M.G., He, Y., Gale Jr., M., 2002. Viruses and interferon: a fight for supremacy. Nat. Rev. Immunol. 2, 675–687.
Lecellier, C.H., Dunoyer, P., Arar, K., Lehmann-Che, J., Eyquem, S., Himber, C., Saib, A., Voinnet, O., 2005. A cellular microRNA mediates antiviral defense in human cells. Science 308, 557–560.
Lee, S.M., Kleiboeker, S.B., 2005. Porcine arterivirus activates the NF-kappaB pathway through IkappaB degradation. Virology 342, 47–59.
Lehmann, S.M., Kruger, C., Park, B., Derkow, K., Rosenberger, K., Baumgart, J., Trimbuch, T., Eom, G., Hinz, M., Kaul, D., Habbel, P., Kalin, R., Franzoni, E., Rybak, A., Nguyen, D., Veh, R., Ninnemann, O., Peters, O., Nitsch, R., Heppner, F.L., Golenbock, D., Schott, E., Ploegh, H.L., Wulczyn, F.G., Lehnardt, S., 2012. An unconventional role for miRNA: let-7 activates Toll-like receptor 7 and causes neurodegeneration. Nat. Neurosci. 15, 827–835.
Li, Y., Fan, X., He, X., Sun, H., Zou, Z., Yuan, H., Xu, H., Wang, C., Shi, X., 2012. MicroRNA-466 l inhibits antiviral innate immune response by targeting interferon-alpha. Cell. Mol. Immunol. 9, 497–502.
Olivieri, F., Rippo, M.R., Prattichizzo, F., Babini, L., Graciotti, L., Recchioni, R., Procopio, A.D., 2013. Toll like receptor signaling in "inflammaging": microRNA as new players. Immun. Ageing: I & A 10, 11.
Otsuka, M., Jing, Q., Georgel, P., New, L., Chen, J., Mols, J., Kang, Y.J., Jiang, Z., Du, X., Cook, R., Das, S.C., Pattnaik, A.K., Beutler, B., Han, J., 2007. Hypersusceptibility to vesicular stomatitis virus infection in Dicer1-deficient mice is due to impaired miR24 and miR93 expression. Immunity 27, 123–134.
Ouda, R., Onomoto, K., Takahasi, K., Edwards, M.R., Kato, H., Yoneyama, M., Fujita, T., 2011. Retinoic acid-inducible gene I-inducible miR-23b inhibits infections by minor group rhinoviruses through down-regulation of the very low density lipoprotein receptor. J. Biol. Chem. 286, 26210–26219.
Papadopoulou, A.S., Dooley, J., Linterman, M.A., Pierson, W., Ucar, O., Kyewski, B., Zuklys, S., Hollander, G.A., Matthys, P., Gray, D.H., De Strooper, B., Liston, A., 2012. The thymic epithelial microRNA network elevates the threshold for infection-associated thymic involution via miR-29a mediated suppression of the IFN-alpha receptor. Nat. Immunol. 13, 181–187.
Parvatiyar, K., Barber, G.N., Harhaj, E.W., 2010. TAX1BP1 and A20 inhibit antiviral signaling by targeting TBK1-IKKi kinases. J. Biol. Chem. 285, 14999–15009.
Pedersen, I.M., Cheng, G., Wieland, S., Volinia, S., Croce, C.M., Chisari, F.V., David, M., 2007. Interferon modulation of cellular microRNAs as an antiviral mechanism. Nature 449, 919–922.
Rani, S., O'Brien, K., Kelleher, F.C., Corcoran, C., Germano, S., Radomski, M.W., Crown, J., O'Driscoll, L., 2011. Isolation of exosomes for subsequent mRNA, MicroRNA, and protein profiling. Methods Mol. Biol. 784, 181–195.
Shi, R., Sun, Y.H., Zhang, X.H., Chiang, V.L., 2012. Poly(T) adapter RT-PCR. Methods Mol. Biol. 822, 53–66.
Shukla, G.C., Singh, J., Barik, S., 2011. MicroRNAs: processing, maturation, target recognition and regulatory functions. Mol. Cell. Pharmacol. 3, 83–92.
Song, L., Liu, H., Gao, S., Jiang, W., Huang, W., 2010. Cellular microRNAs inhibit replication of the H1N1 influenza A virus in infected cells. J. Virol. 84, 8849–8860.
Sun, Y., Han, M., Kim, C., Calvert, J.G., Yoo, D., 2012. Interplay between interferon-mediated innate immunity and porcine reproductive and respiratory syndrome virus. Viruses 4, 424–446.
Triboulet, R., Mari, B., Lin, Y.L., Chable-Bessia, C., Bennasser, Y., Lebrigand, K., Cardinaud, B., Maurin, T., Barbry, P., Baillat, V., Reynes, J., Corbeau, P., Jeang, K.T., Benkirane, M., 2007. Suppression of microRNA-silencing pathway by HIV-1 during virus replication. Science 315, 1579–1582.
Verstrepen, L., Verhelst, K., Carpentier, I., Beyaert, R., 2011. TAX1BP1, a ubiquitin-binding adapter protein in innate immunity and beyond. Trends Biochem. Sci. 36, 347–354.
Wang, P., Hou, J., Lin, L., Wang, C., Liu, X., Li, D., Ma, F., Wang, Z., Cao, X., 2010a. Inducible microRNA-155 feedback promotes type I IFN signaling in antiviral innate immunity by targeting suppressor of cytokine signaling 1. J. Immunol. 185, 6226–6233.
Wang, W.X., Wilfred, B.R., Hu, Y., Stromberg, A.J., Nelson, P.T., 2010b. Anti-Argonaute RIP-Chip shows that miRNA transfections alter global patterns of mRNA recruitment to microribonucleoprotein complexes. RNA 16, 394–404.
Wensvoort, G., de Kluyver, E.P., Pol, J.M., Wagenaar, F., Moormann, R.J., Hulst, M.M., Bloemraad, R., den Besten, A., Zetstra, T., Terpstra, C., 1992. Lelystad virus, the cause of porcine epidemic abortion and respiratory syndrome: a review of mystery swine disease research at Lelystad. Vet. Microbiol. 33, 185–193.
Witwer, K.W., Sisk, J.M., Gama, L., Clements, J.E., 2010. MicroRNA regulation of IFN-beta protein expression: rapid and sensitive modulation of the innate immune response. J. Immunol. 184, 2369–2376.
Yoshikawa, T., Takata, A., Otsuka, M., Kishikawa, T., Kojima, K., Yoshida, H., Koike, K., 2012. Silencing of microRNA-122 enhances interferon-alpha signaling in the liver through regulating SOCS3 promoter methylation. Sci. Rep. 2, 637.
Zhang, L., Bai, J., Liu, J., Wang, X., Li, Y., Jiang, P., 2013a. Toll-like receptor ligands enhance the protective effects of vaccination against porcine reproductive and respiratory syndrome virus in swine. Vet. Microbiol. 164, 253–260.
Zhang, L., Liu, J., Bai, J., Du, Y., Wang, X., Liu, X., Jiang, P., 2013b. Poly(I:C) inhibits porcine reproductive and respiratory syndrome virus replication in MARC-145 cells via activation of IFIT3. Antivir. Res.
Zhang, X.H., Zhang, Y.N., Li, H.B., Hu, C.Y., Wang, N., Cao, P.P., Liao, B., Lu, X., Cui, Y.H., Liu, Z., 2012. Overexpression of miR-125b, a novel regulator of innate immunity, in eosinophilic chronic rhinosinusitis with nasal polyps. Am. J. Respir. Crit. Care Med. 185, 140–151.
Zheng, Z., Ke, X., Wang, M., He, S., Li, Q., Zheng, C., Zhang, Z., Liu, Y., Wang, H., 2013. Human microRNA hsa-miR-296-5p suppresses Enterovirus 71 replication by targeting the viral genome. J. Virol.
Zhou, H., Huang, X., Cui, H., Luo, X., Tang, Y., Chen, S., Wu, L., Shen, N., 2010. miR-155 and its star-form partner miR-155* cooperatively regulate type I interferon production by human plasmacytoid dendritic cells. Blood 116, 5885–5894.
Zhou, R., Hu, G., Liu, J., Gong, A.Y., Drescher, K.M., Chen, X.M., 2009. NF-kappaB p65-dependent transactivation of miRNA genes following Cryptosporidium parvum infection stimulates epithelial cell immune responses. PLoS Pathog. 5, e1000681.